Supplementary Material for: Imaging and Ferroelectric Orientation Mapping of Photostriction in a Single Bismuth Ferrite Nanocrystal

Ahmed H. Mokhtar[1*], David Serban[1], Daniel G. Porter[2], Gareth Nisbet[2], Steve Collins[2], Alessandro Bombardi[2], Marcus C. Newton[1]

[1] School of Physics and Astronomy, University of Southampton
[2] Beamline I16, Diamond Light Source

---

1. Materials and Methods

1.1. Synthesis of $BiFeO_3$ Nanocrystals

Nanocrystals of $BiFeO_3$ were synthesized using a bottom-up epitaxial method on a Sapphire R-plane substrate using pulsed laser deposition (PLD). A 248 nm, 20 mJ KrF excimer laser was used to ablate a solid target of $BiFeO_3$ at a temperature of 700°C in vacuum conditions of 10^{-4} mbar and Oxygen partial pressure. An initial slow deposition cycle with short laser cycles is performed to seed the nanocrystal growth which is left to anneal for a few hours. Subsequent faster laser cycles at slightly higher temperature ensures the ablated material condenses at the seed sites. X-ray diffraction measurements confirms a single phase $BiFeO_3$ growth. The particles' size formed a uniform distribution in the 500-1500 nm range.

1.2. Training of Convolutional Neural Network

Simulated Fourier pairs are used during the network training process, wherein the Fourier space objects are forwarded through the network to generate phase and amplitude predictions, which are subsequently compared to ground truth objects using a loss function, L, as in equation S1. Here, L_1 and L_2 represent losses for real space amplitude and phase, respectively. Additionally, L_3 leverages Fourier transforms of predictions to compute losses relative to the square root of input intensities, where the relative weights of these functions are determined by integer parameters α_1, α_2, and α_3. Back-propagation and training spanned 150 epochs using 30000 Fourier pairs which achieved low and consistent loss profile while employing the ADAM optimiser.

$$L_{Train} = \frac{1}{\alpha_1 + \alpha_2 + \alpha_3}[\alpha_1 L_1(A_p, A_g) + \alpha_2 L_2(\phi_p, \phi_g) + \alpha_3 L_3(\sqrt{I_p}, \sqrt{I_g})] \tag{S1}$$

1.3. Q-Vector Orientation Calculation

The following describes how to calculate the Q-vector for a given diffractometer geometry in the laboratory frame of reference. We will consider a 4S+2D diffractometer using two differing (rectilinear) coordinate systems.

The general (right-handed) rotation matrices about each axis, independent of the orientation of a chosen (rectilinear) coordinate system are:

$$R_{\hat{x}}(\theta) = \begin{bmatrix} 1 & 0 & 0 \\ 0 & \cos\theta & -\sin\theta \\ 0 & \sin\theta & \cos\theta \end{bmatrix} \tag{S2}$$

$$R_{\hat{y}}(\theta) = \begin{bmatrix} \cos\theta & 0 & \sin\theta \\ 0 & 1 & 0 \\ -\sin\theta & 0 & \cos\theta \end{bmatrix} \tag{S3}$$

$$R_{\hat{z}}(\theta) = \begin{bmatrix} \cos\theta & -\sin\theta & 0 \\ \sin\theta & \cos\theta & 0 \\ 0 & 0 & 1 \end{bmatrix} \tag{S4}$$

The coordinate system assumes the beam oriented along the positive $\hat{y}$ direction, the $\hat{x}$ direction pointing upwards and $\hat{z}$ direction along the $\hat{x} \times \hat{y}$ direction [1, 2]. Rotations about μ, η, χ and ϕ according this coordinate system are as follows:

$$\begin{aligned} R_\mu(\mu) &= R_{\hat{x}}(\mu) \\ R_\eta(\eta) &= R_{\hat{z}}(-\eta) \quad \text{i.e. left handed} \\ R_\chi(\chi) &= R_{\hat{y}}(\chi) \\ R_\phi(\phi) &= R_{\hat{z}}(-\phi) \quad \text{i.e. left handed} \end{aligned} \tag{S5}$$

To obtain the complete rotation matrix, matrices in equation S5 are multiplied form the outer most circle (μ) to the inner most circle (ϕ). Noting that the X-ray beam ($\mathbf{k}_i$) is aligned along the positive $\hat{y}$ direction with magnitude k,

$$\mathbf{k}_i = \begin{bmatrix} 0 \\ k \\ 0 \end{bmatrix} \tag{S6}$$

the reflected wavevector ($\mathbf{k}_f$) is given by:

$$\mathbf{k}_f = \begin{bmatrix} k_{f\hat{x}} \\ k_{f\hat{y}} \\ k_{f\hat{z}} \end{bmatrix} = R_\mu(\mu) R_\eta(\eta) R_\chi(\chi) R_\phi(\phi) \mathbf{k}_i \tag{S7}$$

Using equations S6 and S7, the **Q**-vector is then obtained in the laboratory frame of reference as:

$$\mathbf{Q} = \mathbf{k}_f - \mathbf{k}_i \tag{S8}$$

The standard coordinate transform in Bonsu[3] however uses a standard 4S+2D diffractometer right handed coordinate system where the X-ray beam is assumed to align along the positive $\hat{z}$ direction, the $\hat{x}$ direction pointing upwards as before, but the $\hat{y}$ direction pointing along the $\hat{z} \times \hat{x}$ direction.

In this system, rotations about μ, η, χ and ϕ are as follows:

$$\begin{aligned} R_\mu(\mu) &= R_{\hat{x}}(\mu) \\ R_\eta(\eta) &= R_{\hat{y}}(\eta) \\ R_\chi(\chi) &= R_{\hat{z}}(\chi) \\ R_\phi(\phi) &= R_{\hat{y}}(\phi) \end{aligned} \tag{S9}$$

The X-ray beam ($\mathbf{k}_i$) is aligned along the positive $\hat{z}$ direction with magnitude k,

$$\mathbf{k}_i = \begin{bmatrix} 0 \\ 0 \\ k \end{bmatrix} \tag{S10}$$

where $k = \frac{4\pi sin(\theta)}{\lambda}$ is the wave vector magnitude.The $\mathbf{Q}$-vector is then obtained in the laboratory frame of reference as before, as shown above.

2. Tables

Polarization	Chi Loss
$45°$	0.093
$22.5°$	0.080
$0°$	0.108
$-22.5°$	0.103
$-45°$	0.076

Table S1. Final Chi loss from the deep learning CNN for each of the reconstructions.

3. Figures

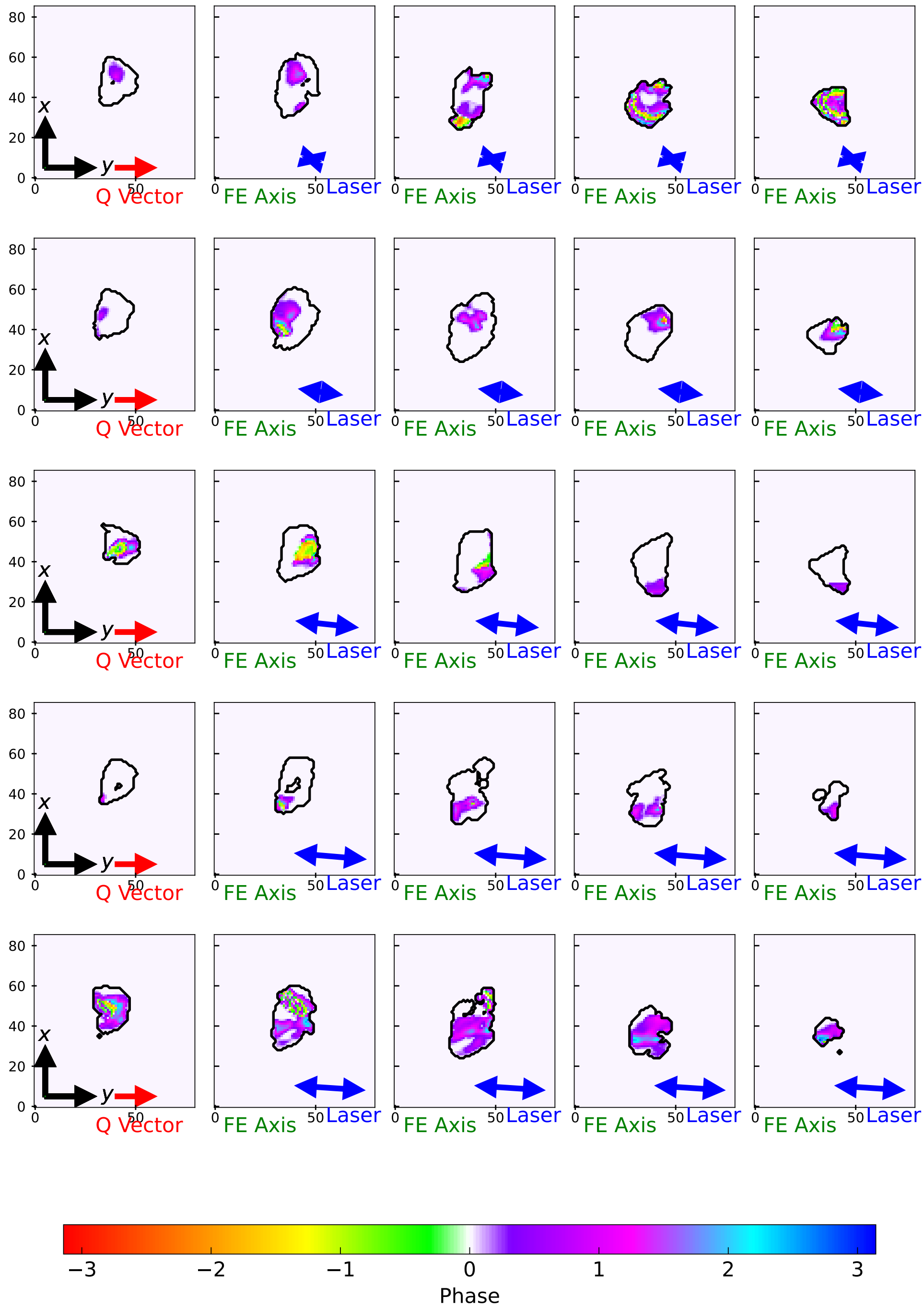

Figure S1. Phase slices in the x-y plane.

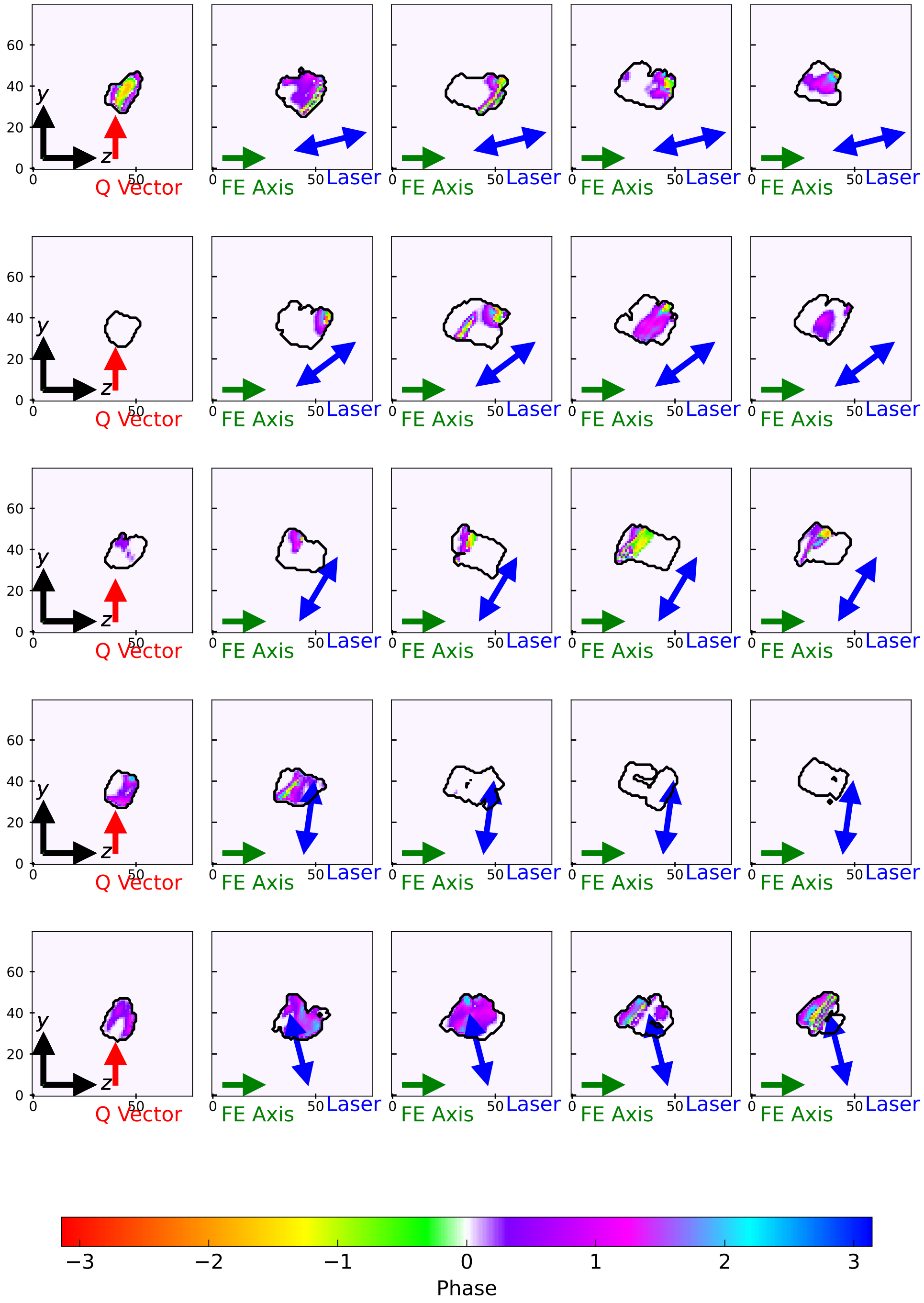

Figure S2. Phase slices in the y-z plane.

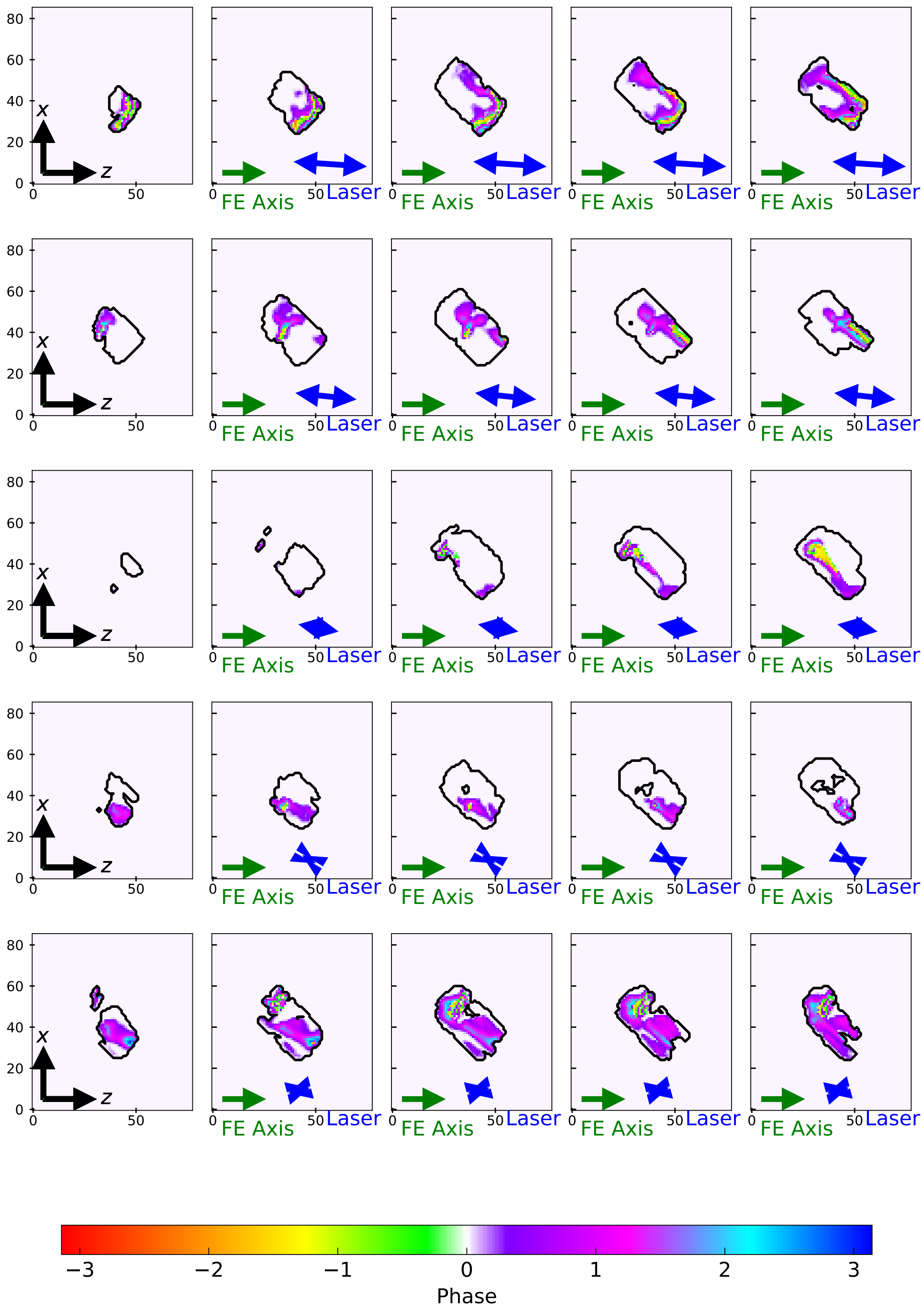

Figure S3. Phase slices in the x-z plane.

(a) (b)

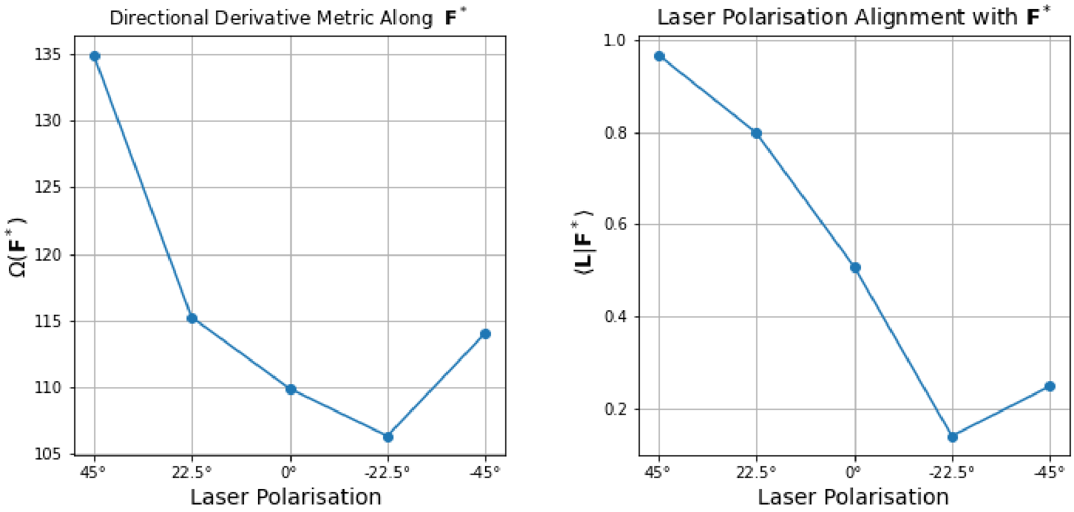

Figure S4. (a) The relationship between the root sum square of the directional derivative metric along the determined ferroelectric axis and the laser polarisation label. (b) The relationship between the inner product of the Laser polarisation direction and the determined ferroelectric axis and the laser polarisation label.

(a) (b)

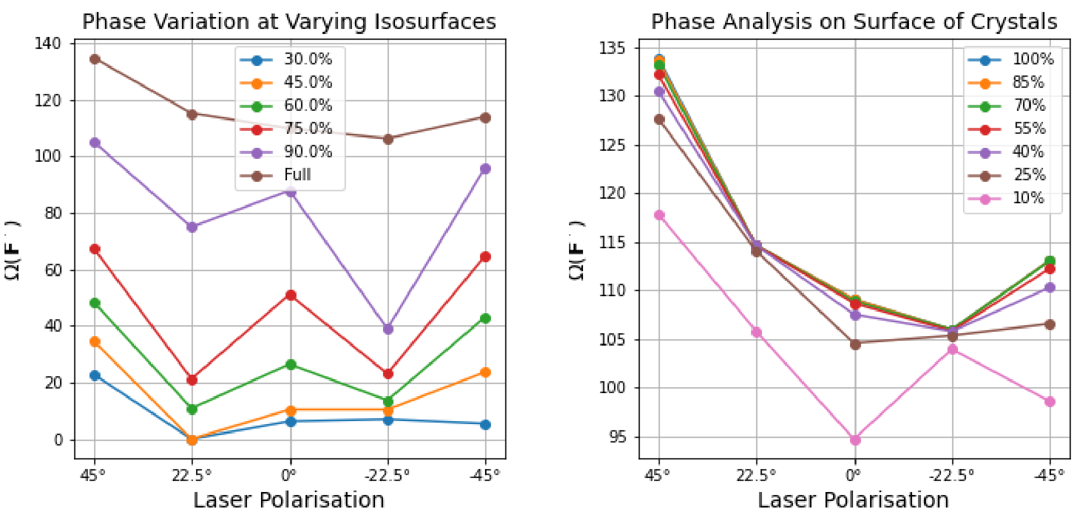

Figure S5. (a) The relationship between the root sum square of the directional derivative metric along the determined ferroelectric axis and the laser polarisation label for different percentages of the crystal's amplitude (b) The relationship between the inner product of the Laser polarisation direction and the determined ferroelectric axis and the laser polarisation label for different shell thicknesses expressed as a percentage of the total amplitude.

References

[1] H. You, "Angle calculations for a '4S+2D' six-circle diffractometer," *Journal of Applied Crystallography*, vol. 32, no. 4, pp. 614–623, Aug 1999. [Online]. Available: https://doi.org/10.1107/S0021889899001223

[2] W. R. Busing and H. A. Levy, "Angle calculations for 3- and 4-circle X-ray and neutron diffractometers," *Acta Crystallographica*, vol. 22, no. 4, pp. 457–464, Apr 1967. [Online]. Available: https://doi.org/10.1107/S0365110X67000970

[3] M. C. Newton, Y. Nishino, and I. K. Robinson, "*Bonsu*: the interactive phase retrieval suite," *Journal of Applied Crystallography*, vol. 45, no. 4, pp. 840–843, Aug 2012. [Online]. Available: https://doi.org/10.1107/S0021889812026751